

Dichotomy in crustal melting on early Mars inferred from antipodal effect

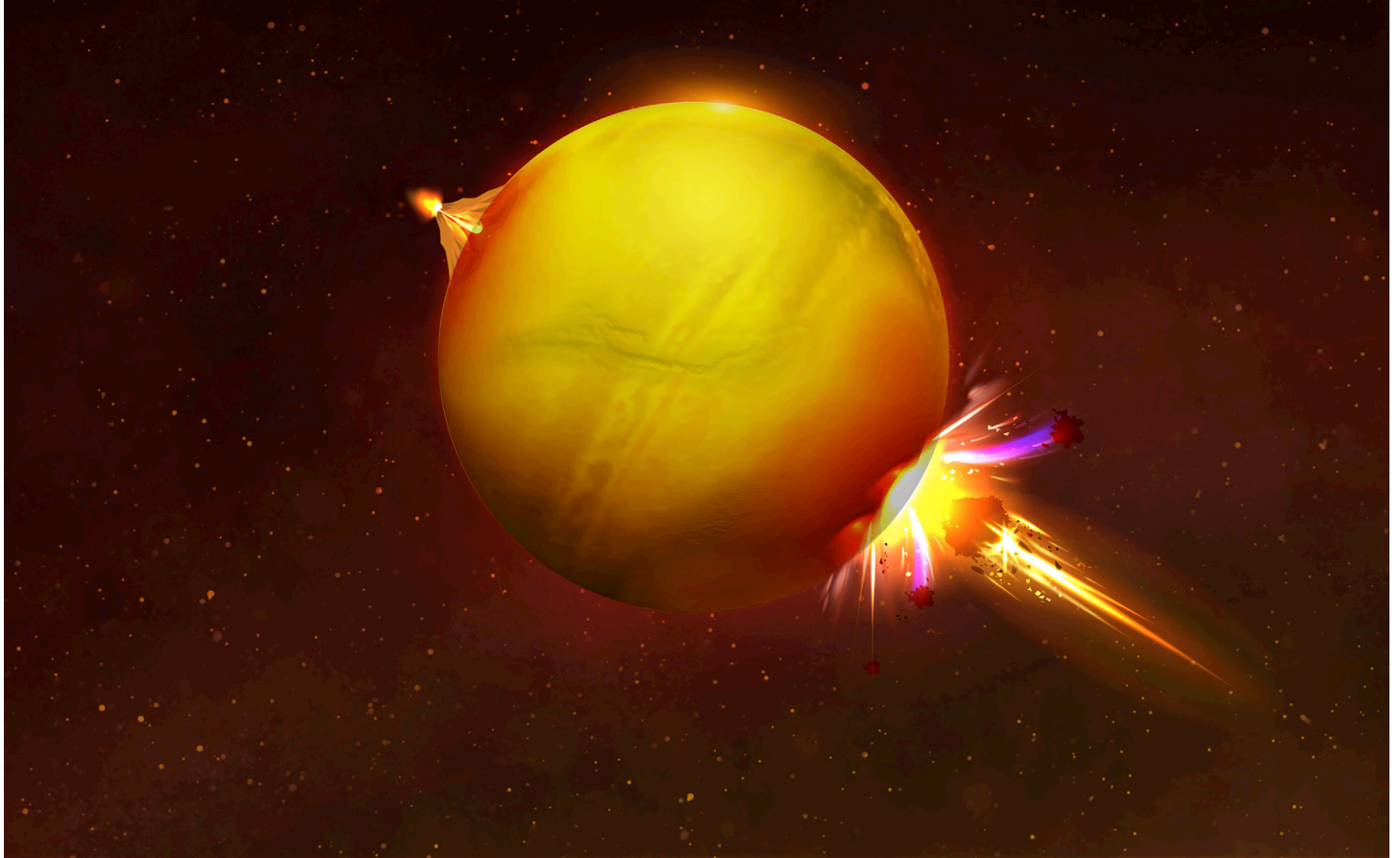
Lei Zhang,^{1,3} Jinhai Zhang,^{1,3,*} and Ross N. Mitchell^{2,*}

*Correspondence: zjh@mail.iggcas.ac.cn (J.Z.); ross.mitchell@mail.iggcas.ac.cn (R.N.M.)

Received: March 30, 2022; Accepted: June 29, 2022; Published Online: July 5, 2022; <https://doi.org/10.1016/j.xinn.2022.100280>

© 2022 The Authors. This is an open access article under the CC BY-NC-ND license (<http://creativecommons.org/licenses/by-nc-nd/4.0/>).

GRAPHICAL ABSTRACT



PUBLIC SUMMARY

- We model the effect of impact-induced seismic waves causing volcanism at its antipode
- A lower southern hemisphere crustal velocity explains the observed Martian antipodes
- The simulation reveals a hemispheric dichotomy in crustal melting on early Mars

Dichotomy in crustal melting on early Mars inferred from antipodal effect

Lei Zhang,^{1,3} Jinhai Zhang,^{1,3,*} and Ross N. Mitchell^{2,*}

¹Key Laboratory of Earth and Planetary Physics, Institute of Geology and Geophysics, Chinese Academy of Sciences, Beijing 100029, China

²State Key Laboratory of Lithospheric Evolution, Institute of Geology and Geophysics, Chinese Academy of Sciences, Beijing 100029, China

³Innovation Academy for Earth Science, Chinese Academy of Sciences, Beijing 100029, China

*Correspondence: zjh@mail.iggcas.ac.cn (J.Z.); ross.mitchell@mail.iggcas.ac.cn (R.N.M.)

Received: March 30, 2022; Accepted: June 29, 2022; Published Online: July 5, 2022; <https://doi.org/10.1016/j.xinn.2022.100280>

© 2022 The Authors. This is an open access article under the CC BY-NC-ND license (<http://creativecommons.org/licenses/by-nc-nd/4.0/>).

Citation: Zhang L., Zhang J., and Mitchell R.N. (2022). Dichotomy in crustal melting on early Mars inferred from antipodal effect. *The Innovation* 3(5), 100280.

The Martian crustal dichotomy (MCD) between the southern highlands and the northern lowlands is the planet's most ancient crustal structure, but its origins and evolution remain enigmatic. Understanding of the MCD comes largely from present-day and shallow crustal constraints. Lacking ancient and deeper constraints, hypotheses for the origin of the MCD range from an early giant impact, partial melting from sustained mantle convection, or some combination. We investigate with seismological modeling the best-preserved case of the “antipodal effect”—energy from an impact that concentrates and induces uplift and fracturing promoting volcanism at its antipode—the Hellas crater and the Alba Patera volcano on Mars. The volcano is latitudinally offset $\sim 2^\circ$ (~ 119 km) from the expected antipode, and we explore whether the MCD can explain this deflection. Variations across the MCD in topography, thickness, and composition have only minor effects. Simulations capable of sufficiently decelerating southern surface waves require the presence of 2%–5% more partial melt in the southern highlands. As the age of impact ca. 4 billion years ago post-dates the formation of the MCD, our partial melting results thus imply that, with or without an early giant impact, the MCD was modified by mantle convection in order to supply enough heat for crustal melts for several hundreds of millions of years after Mars formation.

INTRODUCTION

The Martian crustal dichotomy¹ (MCD) is expressed in many respects (cratering, topography, crustal thickness, and magnetization), but with such present-day observations, it is difficult to infer how ancient Martian geodynamics operated. Thus, understanding the origin and early evolution of the MCD is severely limited. Based on cratering, the highly-cratered southern highlands are likely older than the relatively smooth northern lowlands, but their contrasting magnetizations² has also been interpreted in terms of a single-hemisphere dynamo that would allow the northern and southern crusts to have formed at the same time.³ Appreciable late-stage magmatism occurred in the vast Tharsis magmatic province, but this post-dates the MCD, and mostly lacking magnetization,² much of Tharsis also post-dates the shutdown of the Martian dynamo that presumably had been generated by core-mantle boundary heat flux⁴ due to mantle convection.⁵ Although mantle convection has been invoked by some to explain the MCD,^{5,6} other models invoking a giant impact origin do not require it.⁷ Thus, although the MCD is known to be Mars's oldest crustal structure, much of the geodynamics of how it formed and whether it was related to mantle convection remain unknown. Insights into the crustal dynamics of the early MCD, if made available, could inform the earliest Martian geodynamics and assess whether mantle convection was important in the formation of the MCD or not.

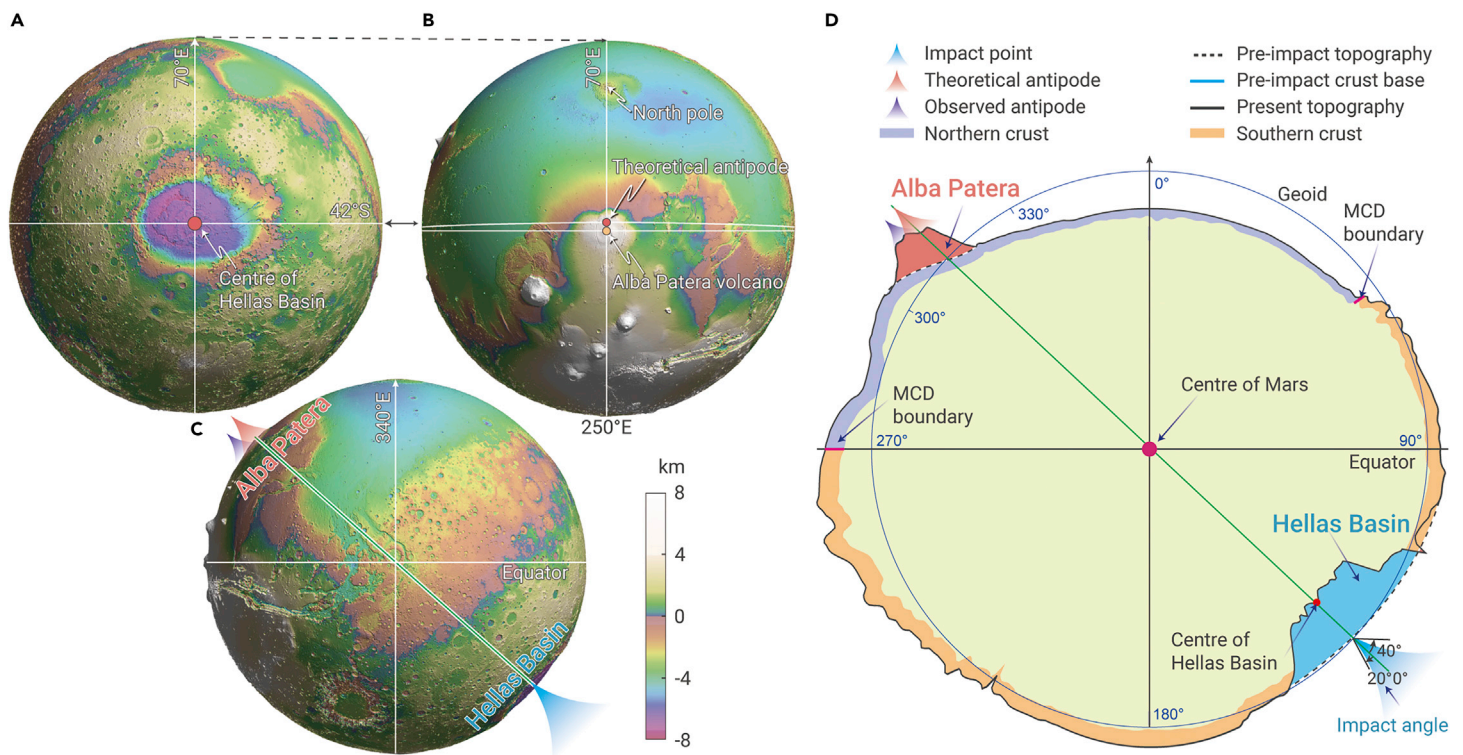


Figure 1. The Hellas basin–Alba Patera antipodal effect on Mars (A) Topographic map centered on Hellas basin (42°S, 70°E). (B) Topographic map centered on the theoretical antipode (42°N, 250°E), where the center of the Alba Patera volcano (the observed antipode) is located $\sim 2^\circ$ (~ 119 km) to the south of the theoretical antipode. (C) Topographic map with north up. (D) Two-dimensional model cross section of (C) along the meridian of 70°E and 250°E. With the North Pole set to have an azimuth of 0°, the impacting point is located at an azimuth of 132°, and its theoretical antipode is at 312°. The observed antipode is located at 310.2°. The topography and crustal thickness of the Martian crustal dichotomy are magnified by 100 and 3 times, respectively, with the geoid shown for reference. The topography around the Hellas basin (purple) and Alba Patera (yellow) is artificially flattened to model the terrain before the impacting.

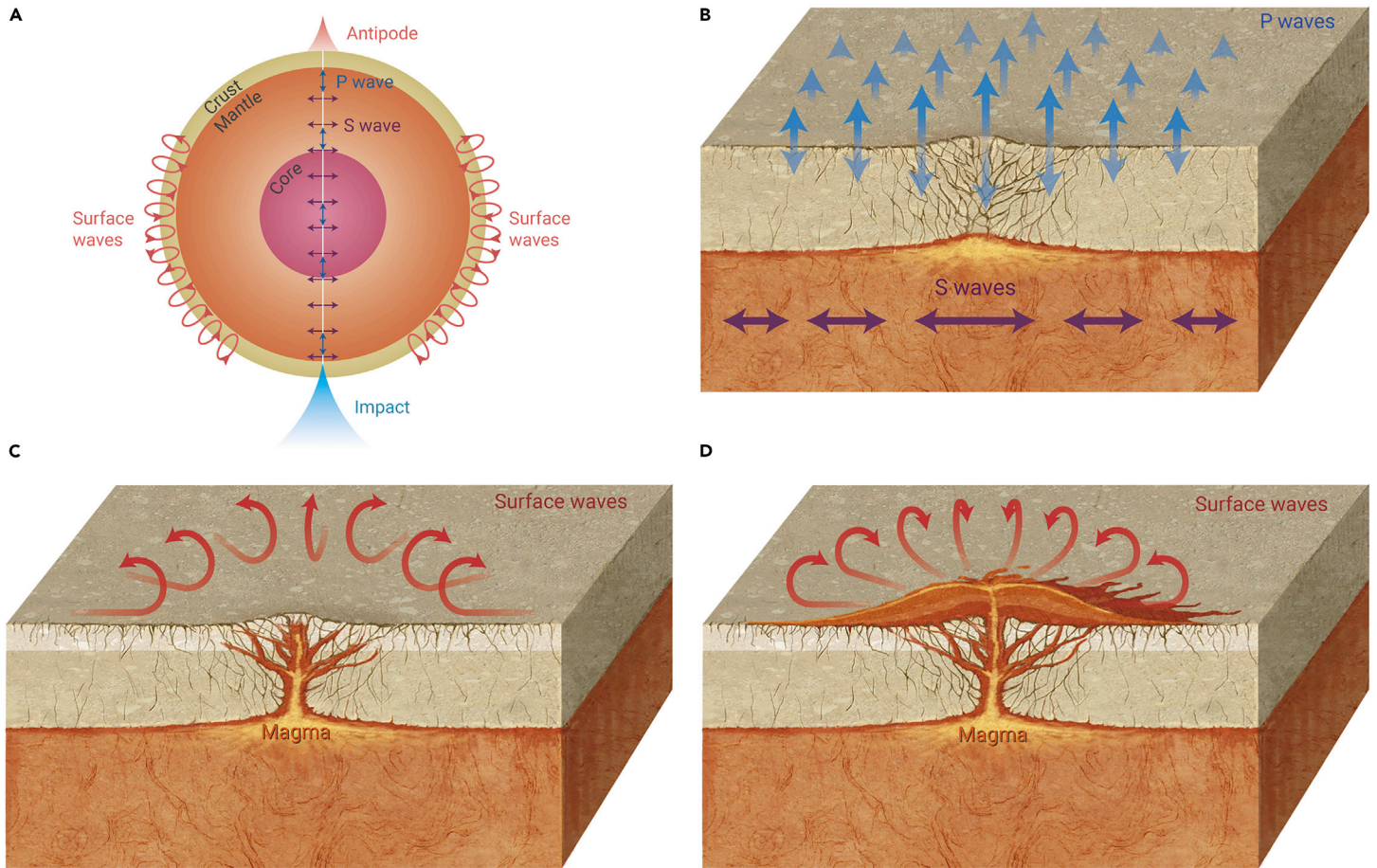


Figure 2. Impact-induced volcanism due to the antipodal effect (A) Cross section depicting the antipodal effect as body waves travel through the core and surface waves travel around the globe surface, and both types of waves finally converge at the antipode. (B) Body waves cause localized domal uplift and some fracturing in the region of the antipode. (C) Surface waves cause ground rolling that creates a larger system of fractures. (D) At a subsequent age of impact when melt is present, magmatism uses the system of fractures to form a volcanic edifice at the antipode.

THE HELLAS–ALBA PATERA ANTIPODAL EFFECT

We use seismological modeling of the antipodal effect^{8–10} associated with the large post-accretionary impact of the Hellas basin and the nearly antipodal Alba Patera volcano to investigate the state of the ancient Martian crust (Figure 1). Impacts are not necessarily expected to cause volcanism close to the crater or at the impact antipode unless additional considerations for triggering are considered.^{11,12} Based on crater counting, the Hellas impact is thought to range from 4.1 to 3.8 billion years ago (Ga) in age,^{13,14} potentially making it part of the late heavy bombardment.¹⁵ Based on crater counting and geologic mapping, Alba Patera is a late Hesperian/early Amazonian (ca. 3.2 Ga) volcanic edifice.¹⁶ Although seismically induced volcanism is possible if a magma chamber is already on the verge of eruption, the relative ages in this case would argue against such a scenario. Thus, the younger Tharsis volcanism was focused in the Alba Patera region due to crustal pre-conditioning by uplift and fracturing from the antipodal effect of the earlier Hellas impact. Subsequent magmatism would occur in the region antipodal to impact according to the uplift (dominantly P and S waves) and fracturing (dominantly surface waves) scenario outlined in Figure 2. The fact that Alba Patera is the farthest large volcano from the center of the Tharsis magmatic province (Figure 1) supports the idea that its emplacement was abetted by such pre-existing fractures. Notably, there is a $\sim 2^\circ$ (~ 119 km) offset between the volcanic center of Alba Patera and the theoretical antipode of the central uplift of the Hellas basin (Figure 1). We explore whether the observed slight deflection of the antipodal effect can be explained by the nature of the MCD at that time.

IMPACT-INDUCED SEISMIC WAVES ON MARS

In an attempt to explain the deviation of the antipodal effect, we take a conservative approach invoking simple explanations at first and only invoke more complex explanations if required. Even before invoking any feature of the MCD,

we explore whether impact angle alone can explain the deviation. Based on the results from numerical modeling (supplemental Figures 1 and 2) using the spectral element method,^{17,18} it turns out that the location of the impact-induced region of uplift and fracturing is always precisely at the antipode, irrespective of whether the impact angle is 0° , 20° , or 40° (Figure 3). We also test a three-dimensional (3D) global-impact-induced seismic wave simulation of the Hellas–Alba antipode. The simulation shows that based on a present-day Mars model, though affected by topography, the surface waves propagate symmetrically and thus concentrate approximately at the exact antipode of the Hellas basin (supplemental Figure 4). This 3D result thus indicates that we can use 2D profiles to avoid computationally intensive 3D forward-modeling simulations for investigation of the MCD on early Mars. Then, we use a 2D radially layered model¹⁹ (supplemental Figures 1 and 2; supplemental Table 1) to assess the effect of impact angles on seismic waves.^{17–20} Martian plate tectonics²¹ occurring after impacting could explain the deflection, but such evidence is limited and contentious; furthermore, the sense of tectonic motion speculated for Alba Patera,²¹ if indeed plate tectonics were operational on Mars, would have moved the volcano in both longitude and latitude, but there is almost no deviation in longitude for the observed antipode (Figure 1). Also, Mars's mantle and core are usually considered radially symmetric in velocity structure, thus body waves mainly propagating through the interior would not affect the antipode position (Figure 2). Therefore, we focus on the surface waves by investigating their asymmetric propagation in the Martian crust and energy concentration around the region of the antipode.

A uniform crustal thickness yields energy at the theoretical antipode and cannot explain the deflection (Figure 4A). Thus, we take the current Martian topography into account in our experiments by calculating the local distribution of relative energy intensity (supplemental Figure 5) near the antipode. The results show that topography contributes only 0.05° , or a

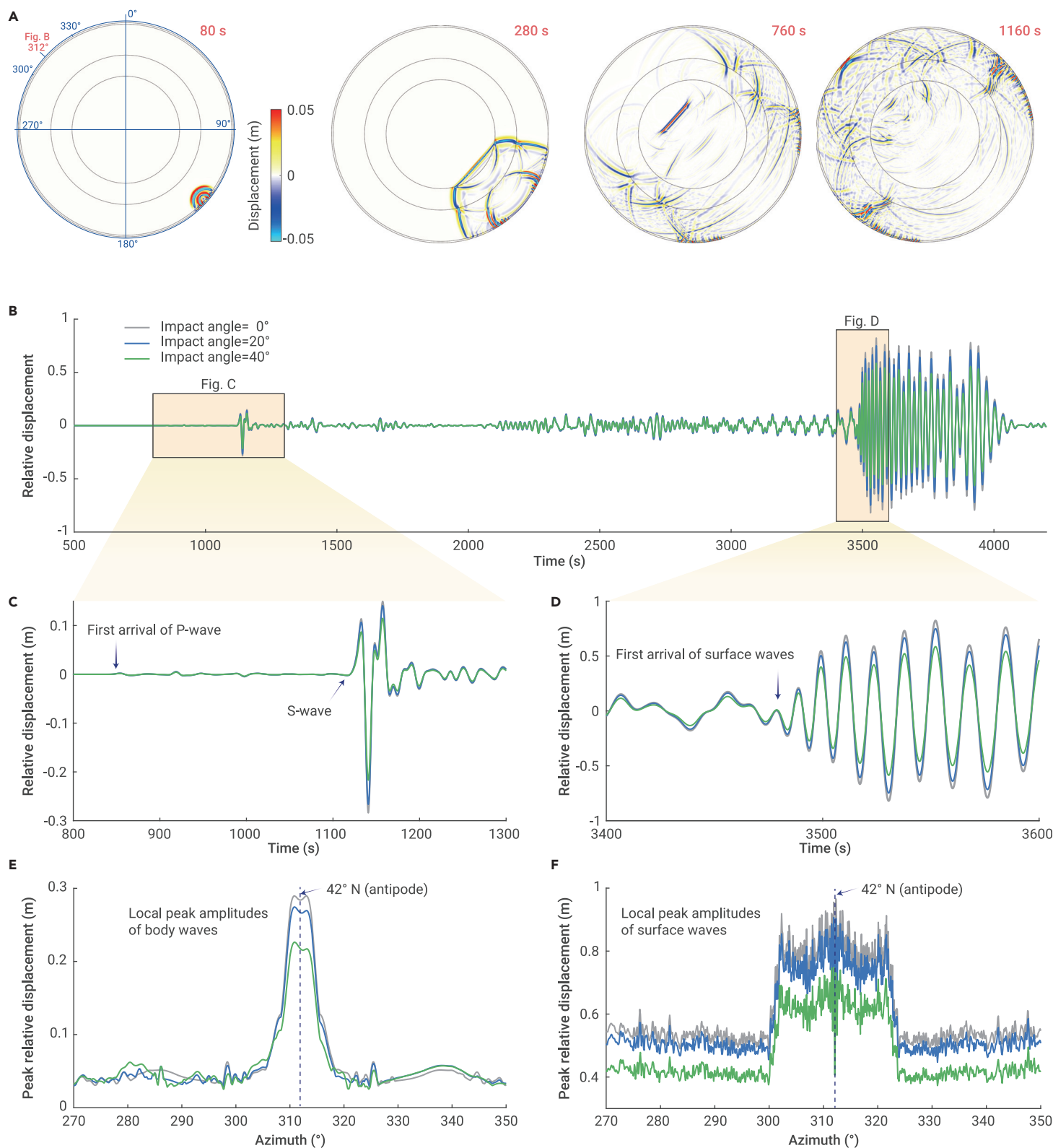


Figure 3. Synthetic impact-induced seismic waves (A) Representative snapshots of radial displacement wavefields. See more snapshots in [supplemental Figure 3](#). (B–D) present radial waveforms and their amplitude distribution at the theoretical antipodal point (azimuth of 312°) with different impact angles. (B) Comparison of waveforms. (C) Partial enlargement of P-waves. (D) Local peak radial displacement distribution in the body-wave window 500–1500 s near the theoretical antipodal point. (E) Local peak radial displacement distribution in the body-wave window 500–1500 s near the theoretical antipodal point. (F) Local peak radial displacement distribution in the surface wave window 1500–5000 s.

negligible 2.5% of the 2° deviation (Figure 4). Such a small topographic effect on the travel time of surface waves (supplemental Figure 5D) is not surprising provided that the ~5 km relief is small compared with average crustal thickness (~50 km).^{7,22} Our next numerical simulations show that the lateral variation of crustal thickness²² evidently moves the simulated antipode ~7.9° northward, which is much larger than the observed deflec-

tion of the antipodal effect and in the opposite direction to reconcile the offset (Figure 4A and supplemental Figure 6). Therefore, the variable crustal thickness across the MCD is an important aspect for explaining the location of Alba Patera, as the large magnitude of its influence effectively sets the true target deviation to be explained, that is, it increases the apparent deviation of only ~2° to ~7.9°.

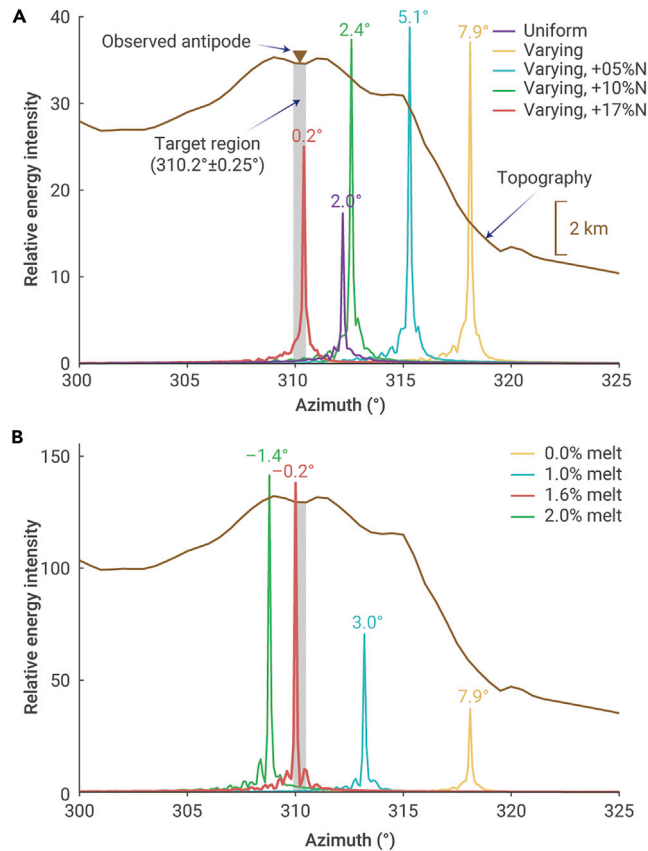


Figure 4. Simulations of the antipodal effect by various crustal parameters The local distribution of relative energy intensity is calculated at the peak amplitudes of surface waves near the antipode (see Figure 3A for the azimuth definition, see [supplemental materials and methods](#) for the calculation details). Topography and crustal thickness are both considered in all cases. The gray shaded region denotes the observed antipode. (A) Simulations with higher crustal velocity (+5%, +10%, and +17%) in the northern crust (Figure 1D). (B) Effects of partial melt in southern upper crust (0–17 km depth) as a percentage more than that in the northern upper crust. More cases with various crustal parameters with hemispheric differences (thickness, compositions, and partial melt) are shown in [supplemental Figure 6](#).

We match the observed deviation by tuning crustal velocity on either side of the MCD. As the paths along the surface to the north and the south have different lengths of arc through the two sides of the MCD (Figure 1D), we must consider two options: the northern lowlands have a higher crustal velocity or the southern highlands have a relatively lower crustal velocity compared with the global crustal model. The matching between the simulated and observed antipodes show that +17% faster crustal velocity in the northern hemisphere or –22% slower crustal velocity in the southern hemisphere can both account for the ~7.9° deviation (including the effects of topography and MCD crustal thickness; Figure 4 and [supplemental Figure 6](#)). To compensate for such an evident deflection, we consider the possibilities of either contrasting crustal compositions or amounts of partial melt on either side of the MCD.

CONTRAST IN CRUSTAL COMPOSITION

We first consider a strong contrast in crustal composition. As most of the Martian crust is thought to be basalt (dense and seismically fast), the only reasonable compositional parameterizations of the hemispheric crustal velocity anomalies would be invoking bulk compositions in the southern hemisphere that are less dense and seismically slower than basalt. As the magnitudes of the relative crustal velocity anomalies are broadly similar for a slower southern crust and a faster northern crust, and both relate to slowing seismic waves traveling through the southern crust, we thus select to parameterize the option of a lower southern crustal velocity anomaly of –22%. It has become apparent that there are more than mafic rocks on Mars. The ChemCam of the Mars Science Laboratory mission deployed at Gale Crater detected multiple distinct soil types

ranging from mafic to felsic compositions.²³ Further evidence of felsic rocks has been argued for on the basis of spectral and aerial imagery²⁴ and geochemistry.^{25,26} Based on the average densities and seismic wave speeds of rocks²⁷ ([supplemental Table 2](#)), we model six possible cases to investigate how a difference of compositions between the southern and northern crusts affects the distribution of relative energy intensity (Table 1). Detailed results of variable crustal compositions, including possible variability at depth (i.e., upper, middle, and lower crusts) are shown in [supplemental Figure 1](#) and Table 1. The results, invoking felsic or intermediate compositions (i.e., andesite or tonalite) in the southern crust (at variable depths) to slow seismic velocities, show that the hemispheric differences in composition exhibit location misfits (i.e., distance from the observed antipode) that range from 2.4° to 8.7°. Therefore, variable crustal compositions across the MCD can only partly explain the formation of Hellas–Alba Patera (H–AP) antipode and are not alone sufficient.

PARTIAL MELTING ACROSS THE CRUSTAL DICHOTOMY

We further consider whether the presence of relatively more melt in the southern crust can cause the crustal velocity anomaly. Provided the old age of the Hellas impact, some degree of melt in the crust is to be expected as a large percentage of the Martian crust, such as the vast Tharsis magmatic province, was generated by post-Hellas magmatism. The presence of 1% melt slows seismic velocities by –7.9% for S-wave speed and –3.6% of P-wave speed.²⁸ We model nine cases to investigate the effect of crustal partial melt on the distribution of relative energy intensity (Table 1). More cases are investigated with and without variable crustal composition as a sensitivity test, and detailed results are listed in Table 1. It is apparent that the crustal partial melt can account for a large portion of the observed deflection ([supplemental Figure 6](#)). For example, ~1.6% melt in the southern upper crust can well represent the relative energy intensity (simulated antipode) around the observed antipode (center of Alba Patera). The best and simplest explanation for the H–AP antipode is that ~1.6% more melt existed in the southern than in the northern upper crust at the age of the Hellas impact at ca. 4 Ga. As a sensitivity test for our result for the 2D profile we use (Figure 1), we picked out six additional 2D planes and attained essentially identical results ([supplemental Figure 7](#)). This demonstrates that our results are independent of the 2D plane analyzed and are supported by any given cross section of the planet ([supplemental Figure 8](#)).

The largest uncertainty in our study is the precise impact location. To be clear, this is not how impact angle affects the antipodal effect (discussed early), but how impact angle affects the structural formation of the impact crater and therefore our ability to deduce the precise point of impact away from which seismic waves traveled. Both laboratory impact experiments and numerical modeling indicate that the antipodal effect of an impact is located antipodal to the first contact point of the impact, which is only the same as the center of the impact basin for vertical impacts.²⁹ For a near-vertical impact angle of 30° (where vertical is 0°), the offset between the first contact point of the impact and the resulting crater center is ~10°.²⁹ The impact angle of Hellas Basin is unknown, with even the suggestion of a double impact.³⁰ The elliptical shape of the crater and the asymmetry of its topography and thickness of the ejecta blankets on the northwest and southeast sides of the crater have been interpreted as resulting from an oblique impact.^{31,32} Nonetheless, elliptical impact basins, particularly for such large impacts as Hellas (the largest on Mars), may alternatively be simply attributed to planetary curvature.³³ Furthermore, the ellipticity of Hellas is notably smaller than the South Pole–Aitkin basin, the largest impact crater on the Moon. We tested the sensitivity of our results to a potential offset of the first point of contact from the crater center. Firstly, although Hellas basin is large, its crater rim to the northwest (the suspected up-range direction in the event of an oblique impact) is <10° away, and given the large diameter of the large impact was likely ~230 km (1/10 the crater diameter), the range of possible locations of the first point of impact implies that the impact angle was nearly vertical (<30°). Secondly, when we offset the impact point in incremental amounts (1°, 2°, 4°, and 8.4°) to the northwest from the crater center, we find that none of the potential offsets reproduce the theoretical antipode, and they actually shift the antipode in the wrong direction to solve the problem ([supplemental Figure 8](#)). Thus, our results are robust given the size and nature of this uncertainty and, furthermore, settle the debate over the

Table 1. Different crust models

Description	Case #	North			South			Deviation (°)
		U	M	L	U	M	L	
Compositions (Northern crust: B, G, and P/Du)	11	B	G	P/Du	A	G	P/Du	-6.5
	12	B	G	P/Du	A + 1%	G + 1%	P/Du + 1%	-12.4
	13	B	G	P/Du	A + 2%	G + 2%	P/Du + 2%	-12.4
	14	B	G	P/Du	B	T	P/Du	-6.2
	15	B	G	P/Du	B + 1%	T + 1%	P/Du + 1%	-10.2
	16	B	G	P/Du	B + 2%	T + 2%	P/Du + 2%	-11.5
	17	B	G	P/Du	A	T	P/Du	-8.7
	18	B	G	P/Du	A + 1%	T + 1%	P/Du + 1%	-12.3
	19	B	G	P/Du	A + 2%	T + 2%	P/Du + 2%	-13.0
Compositions (Northern crust: D, D, and D)	21	D	D	D	A	D	D	3.1
	22	D	D	D	A + 1%	D + 1%	D + 1%	0.8
	23	D	D	D	A + 2%	D + 2%	D + 2%	-1.9
	24	D	D	D	B	T	D	5.5
	25	D	D	D	B + 1%	T + 1%	D + 1%	2.1
	26	D	D	D	B + 2%	T + 2%	D + 2%	0.4
	27	D	D	D	A	T	D	2.4
	28	D	D	D	A + 1%	T + 1%	D + 1%	-0.3
	29	D	D	D	A + 2%	T + 2%	D + 2%	-3.5
Partial melt ratios for southern crust	30	D	D	D	D	D	D	7.9
	31	D	D	D	D + 1%	D	D	3.0
	32	D	D	D	D + 1%	D + 1%	D	5.1
	33	D	D	D	D + 1%	D + 1%	D + 1%	5.5
	34	D	D	D	D + 2%	D	D	-1.4
	35	D	D	D	D + 2%	D + 2%	D	3.2
	36	D	D	D	D + 2%	D + 2%	D + 2%	3.6
	37	D	D	D	D	D	D + 1%	7.5
	38	D	D	D	D	D	D + 2%	7.5
	39	D	D	D	D + 1.6%	D	D	-0.2
Partial melt ratios for A-E antipode	40	D	D	D	D	D	D	-27.8
	41	D	D	D	D + 1%	D	D	-25.8
	42	D	D	D	D + 2%	D	D	-21.6
	43	D	D	D	D + 3%	D	D	-15.7
	44	D	D	D	D + 4%	D	D	-8.7
	45	D	D	D	D + 5%	D	D	2.5
	46	D	D	D	D + 4.8%	D	D	-0.1

See [supplemental Table 2](#) for compositional abbreviations. U, upper crust, ~16.7 km; M, middle crust, ~16.7 km; L, lower crust, ~16.7 km. Every 1% melting indicates 7.9% reduction for S wave velocity (V_s) and 3.6% reduction for P wave velocity (V_p) and density.²⁸ Default Martian crustal composition (D), velocities of basalt (B), Gabbro (G), andesite (A), tonalite (T), pyroxinite (P), dunite (Du), pyroxinite/dunite (P/Du) are obtained from the previous study (see Table S1). Percentages in the table indicate melt ratios.

Hellas impacting scenario: only one impact from a near-vertical impact is required.

To double-check our result for the H-AP antipode, we further explored other antipodal sets of impacts and volcanos as independent tests. There are two other large, post-accretionary impact basins on Mars,³⁴ the Argyre and Isidis bas-

sins. The Isidis basin is the smallest of the three and is not obviously associated with a near-antipodal volcano. The Argye basin is nearly antipodal to Elysium Mons (A-EM antipode; [supplemental Figure 9](#)), but the observed deviation of the antipodal effect is large (~25.5°). In terms of the sense of the deviation, Elysium Mons is indeed south of the theoretical antipode along the path that

seismic waves would have traveled predominantly through the southern hemisphere (supplemental Figure 2B). Thus, the A–EM deflection, however larger, is consistent with the relative sense of the crustal velocity anomalies inferred from the H–AP antipode. Our model of the A–EM antipode suggests that ~4.8% melt existed in the southern upper crust at the age of the Argyre impact (supplemental Figure 9; Table 1). Both the H–AP and A–EM antipodes can be well explained by relatively more partial melt in the southern upper crust of Mars at the time of this post-accretionary bombardment. While the percentages of melt predicted for the two antipodes are broadly consistent, their factor of 3 difference (~4.8% versus ~1.6%) may be attributable to heterogeneity in the distribution of melt in the southern hemisphere, as the two antipodal effects followed different great-circle paths (Figure 1 and supplemental Figure 9) and/or the two impacts were different enough in age to document a change in melt volume on early Mars.

The antipodal effect during the ca. 4 Ga post-accretionary bombardment provides a unique snapshot in time and at deep crustal levels of the geodynamics of the ancient crust of Mars. As more becomes known about the composition of the Martian crust, our results for the percentage of melt can be refined. However, provided that crustal composition has only a minor effect and that similar degrees of melt yielded similar misfits with or without variable compositions, our melt results are unlikely to change considerably. The percentage of melts invoked here may seem large but can be considered reasonable for several reasons. Given the antiquity of the antipodal effect constraints, higher mantle temperatures would have been associated with more melting, akin to Archean Earth with much a greater percentage of melts than today.³⁵ Also, provided evidence for Noachian surface water on Mars,³⁶ upper crustal hydration could have lowered solidus temperatures and increased the presence of melt at shallower depths than otherwise would have been permitted.³⁷ The antipodal effect thus offers a unique window into the geodynamics of ancient Mars and reveals a hemispheric dichotomy in crustal melting during early Noachian time. With or without an early giant impact, the crustal architecture of the MCD was modified by appreciable amounts of crustal melting sustained by heat flux from mantle convection for billions of years after planetary formation.

REFERENCES

- Watters, T.R., McGovern, P.J., and Irwin, R.P. (2007). Hemispheres apart: the crustal dichotomy on Mars. *Annu. Rev. Earth Planet Sci.* **35**, 621–652.
- Acuna, M.H., Connerney, J.E.P., Ness, N.F., Lin, R.P., Mitchell, D., Carlson, C.W., McFadden, J., Anderson, K.A., Reme, H., Mazelle, C., et al. (1999). Global distribution of crustal magnetization discovered by the Mars global surveyor MAG/ER experiment. *Science* **284**, 790–793.
- Stanley, S., Elkins-Tanton, L., Zuber, M.T., and Parmentier, E.M. (2008). Mars' paleomagnetic field as the result of a single-hemisphere dynamo. *Science* **321**, 1822–1825.
- Christensen, U.R., Holzwarth, V., and Reiners, A. (2009). Energy flux determines magnetic field strength of planets and stars. *Nature* **457**, 167–169.
- Zhong, S., and Zuber, M.T. (2001). Degree-1 mantle convection and the crustal dichotomy on Mars. *Earth Planet Sci. Lett.* **189**, 75–84.
- Citron, R.I., Manga, M., and Tan, E. (2018). A hybrid origin of the Martian crustal dichotomy: degree-1 convection antipodal to a giant impact. *Earth Planet Sci. Lett.* **491**, 58–66.
- Andrews-Hanna, J.C., Zuber, M.T., and Banerdt, W.B. (2008). The Borealis basin and the origin of the martian crustal dichotomy. *Nature* **453**, 1212–1215.
- Meschede, M.A., Myhrvold, C.L., and Tromp, J. (2011). Antipodal focusing of seismic waves due to large meteorite impacts on Earth. *Geophys. J. Int.* **187**, 529–537.
- Bozdağ, E., Ruan, Y., Methe, N., Khan, A., Leng, K., van Driel, M., Wiecek, M., Rivoldini, A., Larmat, C.S., Giardini, D., et al. (2017). Simulations of seismic wave propagation on Mars. *Space Sci. Rev.* **211**, 571–594.
- Retailleau, L., Shapiro, N.M., Guilbert, J., Campillo, M., and Roux, P. (2014). Antipodal focusing of seismic waves observed with the USArray. *Geophys. J. Int.* **199**, 1030–1042.
- Ivanov, B., and Melosh, H. (2003). Large Scale Impacts and Triggered Volcanism (Third International Conference on Large Meteorite Impacts). <https://ntrs.nasa.gov/citations/20030067062>.
- Ivanov, B., and Melosh, H. (2003). Impacts do not initiate volcanic eruptions: eruptions close to the crater. *Geology* **31**, 869–872.
- Bottke, W.F., and Andrews-Hanna, J.C. (2017). A post-accretionary lull in large impacts on early Mars. *Nat. Geosci.* **10**, 344–348.
- Robbins, S.J., Hynek, B.M., Lillis, R.J., and Bottke, W.F. (2013). Large impact crater histories of Mars: the effect of different model crater age techniques. *Icarus* **225**, 173–184.
- Bottke, W.F., and Norman, M.D. (2017). The late heavy bombardment. *Annu. Rev. Earth Planet Sci.* **45**, 619–647.
- Anderson, R.C., Dohm, J., Haldemann, A., Hare, T., and Baker, V. (2004). Tectonic histories between Alba Patera and Syria planum, Mars. *Icarus* **171**, 31–38.
- Komatitsch, D., Ritsema, J., and Tromp, J. (2002). The spectral-element method, beowulf computing, and global seismology. *Science* **298**, 1737–1742.

- Komatitsch, D., and Tromp, J. (2002). Spectral-element simulations of global seismic wave propagation - I. Validation. *Geophys. J. Int.* **149**, 390–412.
- Anderson, D.L., Miller, W.F., Latham, G.V., Nakamura, Y., Toksöz, M.N., Dainty, A.M., et al. (1977). Seismology on Mars. *J. Geophys. Res.* **82**, 4524–4546.
- Boslough, M., Chael, E., Trucano, T., and Crawford, D. (1995). Axial focusing of energy from a hypervelocity impact on Earth. *Int. J. Impact Eng.* **17**, 99–108.
- Sleep, N.H. (1994). Martian plate tectonics. *J. Geophys. Res.* **99**, 5639.
- Neumann, G.A., Zuber, M.T., Wiecek, M.A., et al. (2004). Crustal structure of Mars from gravity and topography. *J. Geophys. Res.* **109**, E08002.
- Meslin, P.-Y., Gasnault, O., Forni, O., Schröder, S., Cousin, A., Berger, G., Clegg, S.M., Lasue, J., Maurice, S., Sautter, V., et al. (2013). Soil diversity and hydration as observed by ChemCam at Gale Crater, Mars. *Science* **341**, 1238670.
- Wray, J.J., Hansen, S.T., Dufek, J., Swayze, G.A., Murchie, S.L., Seelos, F.P., et al. (2013). Prolonged magmatic activity on Mars inferred from the detection of felsic rocks. *Nat. Geosci.* **6**, 1013–1017.
- Sautter, V., Toplis, M.J., Wiens, R.C., Cousin, A., Fabre, C., Gasnault, O., et al. (2015). In situ evidence for continental crust on early Mars. *Nat. Geosci.* **8**, 605–609.
- Bouvier, L.C., Costa, M.M., Connelly, J.N., Jensen, N.K., Wielandt, D., Storey, M., et al. (2018). Evidence for extremely rapid magma ocean crystallization and crust formation on Mars. *Nature* **558**, 586–589.
- Christensen, N.I., and Mooney, W.D. (1995). Seismic velocity structure and composition of the continental crust: a global view. *J. Geophys. Res.* **100**, 9761–9788.
- Hammond, W.C., and Humphreys, E.D. (2000). Upper mantle seismic wave velocity: effects of realistic partial melt geometries. *J. Geophys. Res.* **105**, 10975–10986.
- Schultz, P.H., and Crawford, D.A. (2011). Origin of nearside structural and geochemical anomalies on the Moon. *Geol. Soc. Am. Spec. Pap.* **477**, 141–159.
- Arkani-Hamed, J. (2010, December). Hellas: a double-impact basin. In *AGU Fall Meeting Abstracts, 2010*, pp. P51A–P1409.
- Tanaka, K.L., and Leonard, G.J. (1995). Geology and landscape evolution of the Hellas region of Mars. *J. Geophys. Res.* **100**, 5407.
- Leonard, G.J., and Tanaka, K.L. (1993). Hellas basin, Mars: formation by oblique impact. In *Lunar and Planetary Science (Lunar and Planetary Inst., Twenty-Fourth Lunar and Planetary Science Conference. Part 2: G-M)* <https://ntrs.nasa.gov/citations/19940011877>.
- Andrews-Hanna, J.C., and Zuber, M.T. (2010). Elliptical craters and basins on the terrestrial planets. *Geol. Soc. Am. Spec. Pap.* **465**, 1–13.
- Williams, D.A., and Greeley, R. (1994). Assessment of antipodal-impact terrains on Mars. *Icarus* **110**, 196–202.
- Keller, C.B., and Schoene, B. (2012). Statistical geochemistry reveals disruption in secular lithospheric evolution about 2.5 Gyr ago. *Nature* **485**, 490–493.
- Di Achille, G., and Hynek, B.M. (2010). Ancient ocean on Mars supported by global distribution of deltas and valleys. *Nat. Geosci.* **3**, 459–463.
- Collins, W.J., Murphy, J.B., Johnson, T.E., and Huang, H.Q. (2020). Critical role of water in the formation of continental crust. *Nat. Geosci.* **13**, 331–338.

ACKNOWLEDGMENTS

The numerical calculations were conducted on the computing facilities at the National Supercomputing Center in Wuxi. The authors thank Y. Chen and W. Li for generating supplemental Figures 1E and 1F. The authors thank the WeChat official account “Institute for Planets” for their help with Figure 2. C.-H. Zhang (Tsinghua University) provided constructive suggestions that improved the manuscript. This research was supported by Key Research Program of the Chinese Academy of Sciences (ZDBS-SSWTL00104), the National Natural Science Foundation of China (41941002 and 41888101), and the China Postdoctoral Science Foundation (2021M703193). The corresponding authors' websites are as follows: Jinhai Zhang (http://sourcecd.igg.cas.cn/cn/zjrck/yjy/201001/t20100119_2728795.htm) and Ross N. Mitchell (http://sourcecd.igg.cas.cn/cn/zjrck/yjy/201912/t20191219_5460988.htm).

AUTHOR CONTRIBUTIONS

Conceptualization, J.Z., R.N.M., and L.Z.; methodology, L.Z.; investigation, R.N.M., L.Z., and J.Z.; visualization, L.Z.; supervision, J.Z. and R.N.M.; writing – original draft, L.Z. and J.Z.; writing – review & editing, R.N.M. and J.Z.

DECLARATION OF INTERESTS

The authors declare no competing interests.

SUPPLEMENTAL INFORMATION

Supplemental information can be found online at <https://doi.org/10.1016/j.xinn.2022.100280>.

LEAD CONTACT WEBSITE

The corresponding authors' websites are as follows: Jinhai Zhang (http://sourcecd.igg.cas.cn/cn/zjrck/yjy/201001/t20100119_2728795.htm) and Ross N. Mitchell (http://sourcecd.igg.cas.cn/cn/zjrck/yjy/201912/t20191219_5460988.htm).